Hindawi
Advances in Civil Engineering
Volume 2023, Article ID 4331735, 12 pages
https://doi.org/10.1155/2023/4331735

Research Article

Simulation Study of New Buckling Restraint Bracing Based on Bayesian Optimization Algorithm to Identify the Parameters of Modified Bouc–Wen Model

Lu Zhao,[1] Tiangang Tu ,[2,3] Sunwei Ding,[2,3] and Xinqiao Liu[2,3]

[1]*Shanghai Polytechnic University, Shanghai 200120, China*
[2]*Shanghai Research Institute of Materials, Shanghai 200437, China*
[3]*Shanghai Energy Dissipation and Shock Absorption Engineering Technology Research Center, Shanghai 200437, China*

Correspondence should be addressed to Tiangang Tu; 804812818@qq.com

Received 29 September 2022; Revised 4 December 2022; Accepted 9 December 2022; Published 3 January 2023

Academic Editor: John Mander

The introduction of new materials can significantly improve the performance of existing dampers, but the constitutive model of new materials is difficult to be obtained in a short time, which makes its numerical simulation difficult. Bouc–Wen–Baber–Noori (BWBN) model can well describe the stress-strain relationship of materials, and it is helpful to introduce new materials into numerical simulation. In this paper, a new high manganese steel material is used to fabricate buckling restrained brace, and based on the improved Transition Markov Chain Monte Carlo (iTMCMC) sampling method and Bayesian reasoning, a new parameter identification of BWBN model is completed; model parameters are introduced into OpenSees to complete the response analysis of the new steel damper in the structure. It provides a new method and approach for introducing new materials into structural seismic resistance and proves its reliability.

1. Introduction

The constitutive model of new materials is of great significance for engineering numerical simulation. Inaccurate constitutive parameters will lead to errors in numerical simulation [1, 2]. BWBN model is not only widely used in reinforced concrete frame structures [3], seismic residual displacement [4, 5], structural health monitoring, and other fields [6, 7], but also to simulate various dampers, such as yielding shear panel device [8], and magnetorheological dampers [9]. The application of BWBN model needs to clarify its parameters first. At present, there are many methods to identify the parameters of BWBN model based on experimental data, such as Genetic algorithm [10, 11], Cuckoo Search Algorithm [12], artificial neural network [13], and Transitional Markov Chain Monte Carlo method [14]. Because of the introduction of new materials, it may be necessary to constantly adjust the model parameters in order to obtain a better fitting effect. However, the parameter identification methods such as genetic algorithm and neural network algorithm cannot provide the possible value probability of parameters, which is not conducive to model updating. Once the BWBN model parameters are found, when the difference between the experimental data and the output of the mathematical model is small enough, the resulting model is regarded as a "good" approximation of the real experimental lag [15]. At the same time, because the improved Bouc–Wen model (BWBN, iTMCMC) can describe several modes matching the response of a series of hysteretic systems, this paper applies it to a "fuse", which is made of elastic-plastic austenitic steel with low stacking fault energy and analyzes its reliability.

Some scholars have compared several design concepts of viscous dampers in building structures [16], and it has been found that the energy-based design strategy provides the best distribution method among a wide group of analyzed design methodologies complying with an equal (target) damping ratio constraint. In addition, some scholars have summarized a variety of algorithms to invert the optimal design parameters of passive dampers in order to achieve the desired performance of buildings [17], Nowadays, an input velocity adjustment method of the critical double impulse was presented for the efficient design of viscous dampers for elastic-plastic moment frames [18]. It can be seen that there are many researches on algorithms for building structure health, but there are certain differences between the parameters of dampers deduced backwards for the purpose of building health and the real parameters obtained from the produced dampers. Such differences may lead to changes in the response of building structures, which will lead to adverse results.

In order to protect buildings on soft soil foundation that are not suitable for seismic isolation technology from earthquake damages, it is necessary to install dampers or supports in the structure that can dissipate energy and have the same redundancy as the building [19–21]. Buckling restrained brace (BRB) is widely used in the field of building damping because of its economy and excellent energy dissipation capacity [22]. Traditional BRBs have poor low cycle fatigue performance, durability, ductility, and other related properties [23, 24], which may lead to serious damage to buildings due to the fact that BRBs cannot achieve the same redundancy with buildings after earthquakes. Some studies have found that, dampers effectively reduce the failure probabilities of the structural frame and the facility components and It shows that the damper with the same redundancy as the building can protect the building from earthquake damage to the greatest extent [25].

2. Modified Bouc–Wen Model

Bouc–Wen model is a smooth hysteretic model represented by differential equations. On the basis of Bouc–Wen model, Wen, Baber, and Noori [26, 27] defined strength, stiffness degradation parameters, and pinching effect function, which expanded the function of Bouc–Wen model (also known as BWBN model). So far, BWBN model is widely used to describe hysteresis in various projects. The schematic diagram of Bouc–Wen single degree of freedom model is shown in Figure 1, and the equation of motion can be expressed by the following equations:

$$m\ddot{x} + c\dot{x} + akx + (1 - a)kz = F(t), \tag{1}$$

$$\dot{z} = \frac{h(z)}{\eta(t)}\left\{\dot{x} - \nu(t)\left(\beta|\dot{x}|z|z|^{n-1} + \gamma\dot{x}|z|^{n}\right)\right\}. \tag{2}$$

In equation (1), a is the ratio of postyield stiffness to preyield elastic stiffness $a = E_P/E$, m is the mass, c is the damping constant, k is the stiffness coefficient, and z is the hysteresis parameter. In equation (2), $\nu(t)$ represents strength degradation, $\nu(t) = 1.0 + \delta_\nu \varepsilon(t)$, $\eta(t)$ represents stiffness degradation, $\eta(t) = 1.0 + \delta_\eta \varepsilon(t)$, and $h(z)$ represents pinch effect.

Some scholars have introduced the derivation process of Bouc–Wen model and the detailed process of parameter identification using traditional Bayesian inference [6, 14]. In this paper, the fourth-order Runge–Kutta method is used to solve the differential equation in the BWBN elastic measurement model as follows:

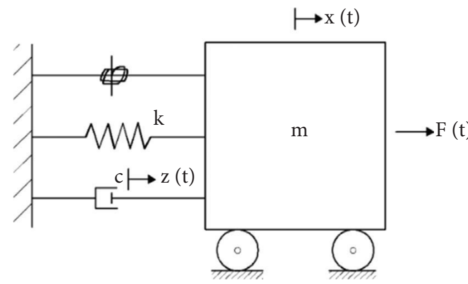

Figure 1: BWBN model diagram.

$$\begin{aligned} y_{n+1} &= y_n + \frac{h}{6}\left(K_1 + 2K_2 + 2K_3 + K_4\right),\\ K_1 &= f\left(x_n, y_n\right),\\ K_2 &= f\left(x_n + \frac{1}{2}h, y_n + \frac{1}{2}hK_1\right),\\ K_3 &= f\left(x_n + \frac{1}{2}h, y_n + \frac{1}{2}hK_2\right),\\ K_4 &= f\left(x_n + h, y_n + hK_3\right), \end{aligned} \tag{3}$$

where $f()$ represents the differential equation of BWBN model, x_n is the displacement in the measured data, $y_n = F(t)$ is the force in the measured data, h is the Runge–Kutta time step, and K_1, K_2, K_3, K_4 are the transfer parameters in Runge–Kutta.

3. Model Updating Techniques

To apply the BWBN model to describe the hysteretic behavior of the system, the first problem is to find better model parameters. The random sampling method can deal with more general situations than the asymptotic approximation method. The parameter identification method based on Bayesian theory can not only give the optimal values of parameters, but also obtain the covariance matrix that quantitatively describes the uncertainty of model parameters. This is of great significance and theoretical value to improve the robustness and accuracy of system identification.

Worden and Hensman [28] explained how the Bayesian method provides the same and more information as the differential evolution algorithm method, and used Markov Chain Monte Carlo (MCMC) and Metropolis–Hastings (MH) techniques to estimate the parameters of the BW model of hysteresis. Cheng et al. [29] replaced Gaussian sampling with differential evolution algorithm to form an improved DE-TMCMC method to identify the parameters of sand constitutive model. Betz et al. [30] provided three ways to improve TMCMC sampling methods. This paper synthesizes the first and third improvement measures, and uses iTMCMC algorithm to identify the parameters of BWBN model. The specific implementation method is shown in the Figure 2.

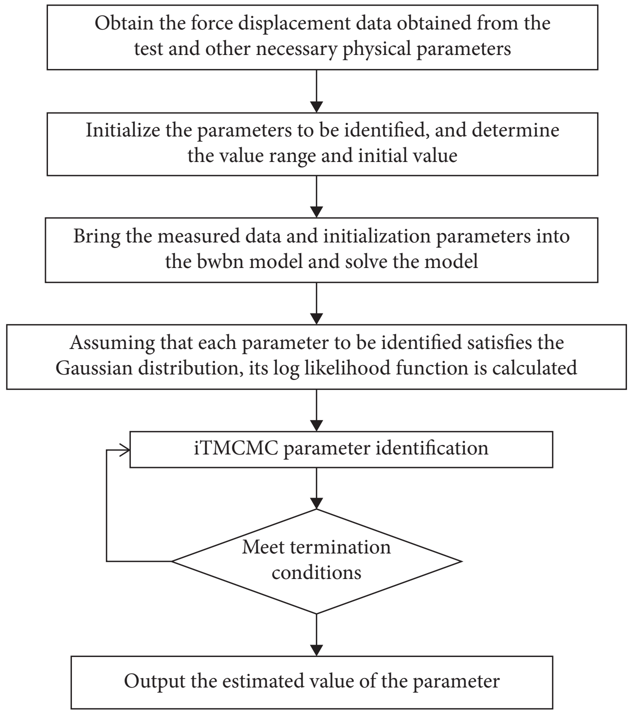

FIGURE 2: Calculation flow chart.

Let θ be the set of uncertain parameters and D represents measured data. The core of parameter estimation using probability idea is to know the probability density distribution (PDF) of parameters. According to Bayesian reasoning, the posterior distribution of the undetermined parameter $P(\theta \mid D) \propto P(D \mid \theta)P(\theta)$ and θ of the undetermined parameters are assumed to be Gaussian distribution with standard deviation of 1, and the mean value of the prior distribution is shown in θ^* in Table 1. The likelihood function of the mean square error (MSE) between the calculated D and the system estimated response of the given parameter θ^* is shown in the following equations:

$$P(D \mid \theta) = \prod_{i=1}^{N} \left(\sigma^2 \sqrt{2\pi}\right)^{-1} \exp\left[-\frac{1}{2\sigma^2} J_{\text{dis}}(\theta, D)^2\right], \quad (4)$$

$$J_{\text{dis}}(\theta, D) = u(i) - \hat{u}(i \mid \theta), \quad (5)$$

where N is the amount of data, σ is the variance between the test displacement and the displacement prediction error calculated by the BWBN model with the current parameter, u is the actual displacement value of the test, and $\hat{u}$ represents the average value of the displacement predicted by the BWBN model with the current parameter. For the convenience of calculation, the log-likelihood function should be used in the actual implementation of iTMCMC.

After obtaining the log-likelihood function, enter iTMCMC sampling, mainly using the first and third improvements proposed by Betz et al. [30], and the main steps are as follows:

(i) Prior distribution and likelihood function of input parameters;

TABLE 1: Parameter sampling range.

Param	$\theta_{\min}$	θ^*	$\theta_{\max}$
α	0.01	0.20	0.30
β	1.00	2.00	4.00
γ	−4.00	−1.00	4.00
n	1.00	1.20	3.00
v_0	0.10	1.20	3.00
δ_v	−2.00	0.40	4.00
A_0	0.50	1.10	3.00
δ_A	−2.00	0.10	3.00
η_0	0.50	1.30	4.00
δ_η	−3.00	0.50	4.00

(ii) Calculate q_j. If $q_j > 1$, let $q_j = 1$, set $i = 0$, and extract $\{\mu_k^0, k = 1, 2, \ldots\ldots, N\}$ samples from the prior distribution.

(iii) The weighting coefficient is calculated for all the samples $\{\mu_k^0, k = 1, 2, \ldots\ldots, N\}$, where $j = 0, \ldots, m$, $0 = q_0 < q_1 < \cdots < q_m = 1$, and $\mu_{(j,k)} = \mu^c_{(j,l)}$.

$$w_{(j,k)} = \left(P\left(\mu^c_{(j,l)} \mid D\right)\right)^{q_j - q_{j-1}}. \quad (6)$$

(iv) Calculate the average value of the following weighting coefficient:

$$S_j = \frac{1}{N_S} \sum_{k=1}^{N_S} w_{(j,k)}. \quad (7)$$

(v) The covariance matrix is calculated, wherein the scaling factor $\beta = 2.4/\sqrt{M}$ is adaptively adjusted as follows:

$$\sum_j = \beta^2 \bullet \sum_{k=1}^{N_S}\left[\frac{w_{(j,k)}}{S_j \cdot N_S}\bullet\left(\mu_{(j-1,k)} - {}^{-}\mu_j\right)\bullet\left(\mu_{(j-1,k)} - \bar{\mu}_j\right)^T\right]. \tag{8}$$

(vi) The index l is randomly selected from the set $\{1, \ldots, N_S\}$ according to the probability $w_{j,l}/\sum_{n=1}^{N_S} w_{(j,n)}$ to obtain μ^c as the initial sample to start the Markov chain. The Gaussian distribution centered on the current sample in the k-th chain and the covariance matrix $\sum_j$ are taken as μ^c suggested distributions. Let R be a sample in a uniform distribution of 0 to 1, if $r \le P_j(\mu^c)/P_j(\mu^c_{(j,l)})$, let $\mu^c_{(j,l)} = \mu^c$. Then, proceed to the following step $\mu_{(j,k)} = \mu^c_{(j,l)}$ and $w_{(j,l)} = (f(\mu^c_{(j,l)} \mid D))^{q_j - q_{j-1}}$;

(vii) If $q_j = 1$, stop the iteration; otherwise, make $j = j + 1$ and continue the cycle from step 1.

The detailed steps can be seen from the three ways of improving TMCMC proposed by Betz et al. [30], and it is proved that the average deviation of evidence estimation obtained by iTMCMC method is small, and its performance is better than that of the original TMCMC method.

4. Experiment of the New Type Buckling Restrained Brace

Buckling restrained braces (BRBs) are widely favored because they have sufficient seismic performance in compression and tension. Dizaj et al. [31] proposed a shortened BRB with low yield and proved that the shortened BRB has lower potential danger. Iwata et al. [32] said that due to the longer and longer duration of the earthquake, it was necessary to study and develop new buckling restrained braces with better fatigue performance and higher energy dissipation capacity, and put forward corresponding opinions from the structure.

This paper studies the identification of mechanical properties of high ductility buckling restrained energy dissipation braces (double stage axial steel damper) made of a new type of austenite steel that Yang et al. [33] of Shanghai Research Institute of materials developed. The ductility coefficient (i.e., the ratio of the ultimate displacement to the yield displacement) of the new two-stage axial steel damper is more than 12, which can realize the energy dissipation and damping effect under different earthquake intensities and achieve the same redundancy failure as the building. The test piece and test principle of high ductility double order buckling restrained brace made of new materials are shown in Figures 3 and 4.

The total length of BRB core plate is 1.5 m, the thickness is 16 mm, C45 concrete is poured in the barrel, and the test loading frequency is 0.05 Hz. Because the core plate is welded by traditional ferritin steel plate and new austenite steel plate, as shown in Figure 5, under cyclic loading, the weld breaks and the strength of the component decreases, thus achieving the purpose of double-stage energy consumption.

Figure 3: Buckling restrained bracings with high ductility.

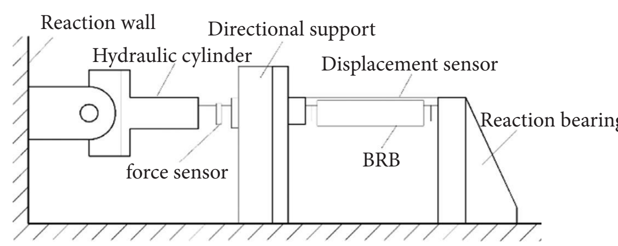

Figure 4: Schematic diagram of test principle.

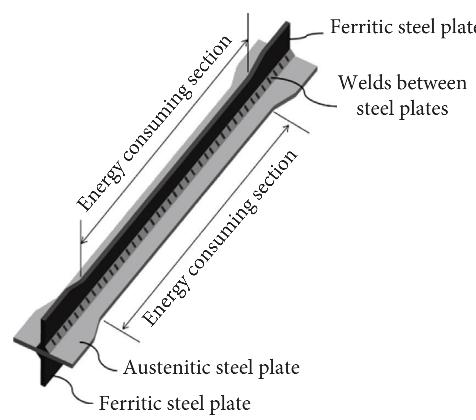

Figure 5: Schematic diagram of double order constraint support.

The traditional BRB core plate material is a low yield ferritin steel, and the fatigue life of ferritin steel is low during cyclic loading deformation. The new austenite steel described in this paper changes the deformation mechanism of the traditional steel, improves the fatigue resistance and ductility of the material, and the new material can miniaturize the buckling restrained brace. In this paper, a miniaturized BRB full-scale test is carried out. The maximum tensile and compressive bearing capacity of the core element after yielding in each loading cycle is not lower than the yield load. The obtained hysteresis curves are shown in Figure 6.

From Figure 6, it shows that the new BRB has almost no stiffness degradation under 30 cycles of cyclic load, and has a certain degree of strength degradation, which meets the requirements of double-order energy consumption. The displacement is within 1/40 range, and a stable, full,

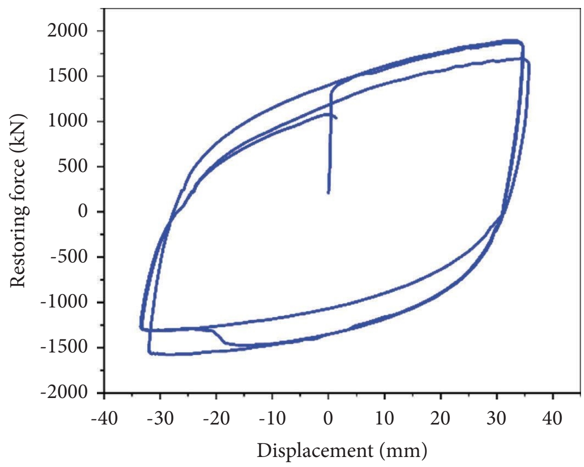

Figure 6: Experimental hysteresis cycles.

repeatable, and nondecaying hysteresis curve of bearing capacity is obtained.

Therefore, it can be seen that the new BRBs has the following advantages:

(1) The axial damper overcomes the shortcomings of the ductility of the traditional buckling restrained brace, maximizes the deformation capacity of the damper, achieves the same seismic redundancy with the main structure, and ensures the energy dissipation in the whole process under the earthquake.

(2) Under the same deformation design, the length of the damper is shorter and easy to install. Through bolt connection, quick replacement and repair after earthquake can be realized.

(3) Based on excellent performance, optimize the main structure, reduce the consumption of traditional concrete and steel, reduce carbon emissions, and significantly improve the seismic performance of buildings to meet the needs of resilient cities.

In order to apply the new type of buckling restrained brace to engineering, it is necessary to conduct simulation analysis on it during design. However, the new product cannot form its constitutive model in a short time, which is unfavorable for engineering application. Different research institutions have different models and parameter identification methods to describe the hysteresis performance of BRB. In terms of models, commonly used models include double (multiple) linear model [34], Ramberg Osgood model [35] and Bouc–Wen model [36]. These models have the advantages of smooth curve, high simulation accuracy, and strong adaptability, but at the same time, these models do not have the characteristics of describing stiffness degradation and strength degradation.

5. Identification

In order to further study the response of the new steel damper in the structure, it is necessary to obtain the constitutive model of the stress-strain relationship of BRB. In recent years, Bayesian model updating technology has been more and more applied to the neighborhood of hysteresis system parameter identification. Ortiz et al. [14] first used Bayesian model updating technology to identify BW model parameter that can simulate degradation effects, and found the parameter set that can accurately reproduce the system response, but did not find the accurate value of the parameters related to BWBN model. Angelikopoulos et al. [37] proposed the X-TMCMC algorithm in 2015, which combines the adaptive Kriging method with the Transitional Markov Chain Monte Carlo (TMCMC) technology to improve the parallel efficiency of the algorithm. In this paper, iTMCMC method is introduced into the parameter identification of BWBN model for the first time, which improves the calculation efficiency and achieves better model updating effect. Based on the original TMCMC method, iTMCMC algorithm mainly makes the following modifications:

(i) Adjust the sample weight after each MCMC step to reduce the average deviation of model evidence estimation

(ii) Apply aging period in MCMC step to improve posterior approximation

(iii) The target distribution scale of MCMC algorithm is adaptively selected to achieve near optimal acceptance rate

iTMCMC is set to the following values: the number of samples in all stages, is set to 1000, the specified threshold of c.o.v. is set to 100%, and the aging parameter is set to 50. Each parameter is sampled independently. If the parameters are related, it is based on the edge transformation of the reconstructed joint distribution (nataf) method. The estimated value of the parameter range is shown in Figure 7.

It is shown from Figure 8 that the identified parameters can make the modified BW model reflect the strength degradation effect and estimate the actual second-order response of the system better. The comparison results show that the theoretical model can well simulate the mechanical performance of the composite damper under cyclic load and can replace the test results for theoretical analysis. The identification method has shown that it can find a parameter set capable of reproducing the system response. The BWBN model is a multimodal function. Although the exact values of the parameters related to the BWBN model are not estimated, the system response evaluated using the estimated parameters is sufficient for simulation purposes. The identification parameters are shown in the Table 2.

Since the hysteretic system to be identified has no pinch effect, this paper does not consider the parameters controlling pinch. The BWBN model is a multimodal function [15], which allows multiple groups of parameters to achieve a good estimation of the system response. At the same time, the existing literature shows that the parameter values of the BWBN model are often in a fixed range [38, 39]. This paper finds that when parameter estimation is carried out by means of probability thinking, the parameter sampling range can be appropriately expanded and the number of sampling points can be appropriately increased to obtain a better parameter set.

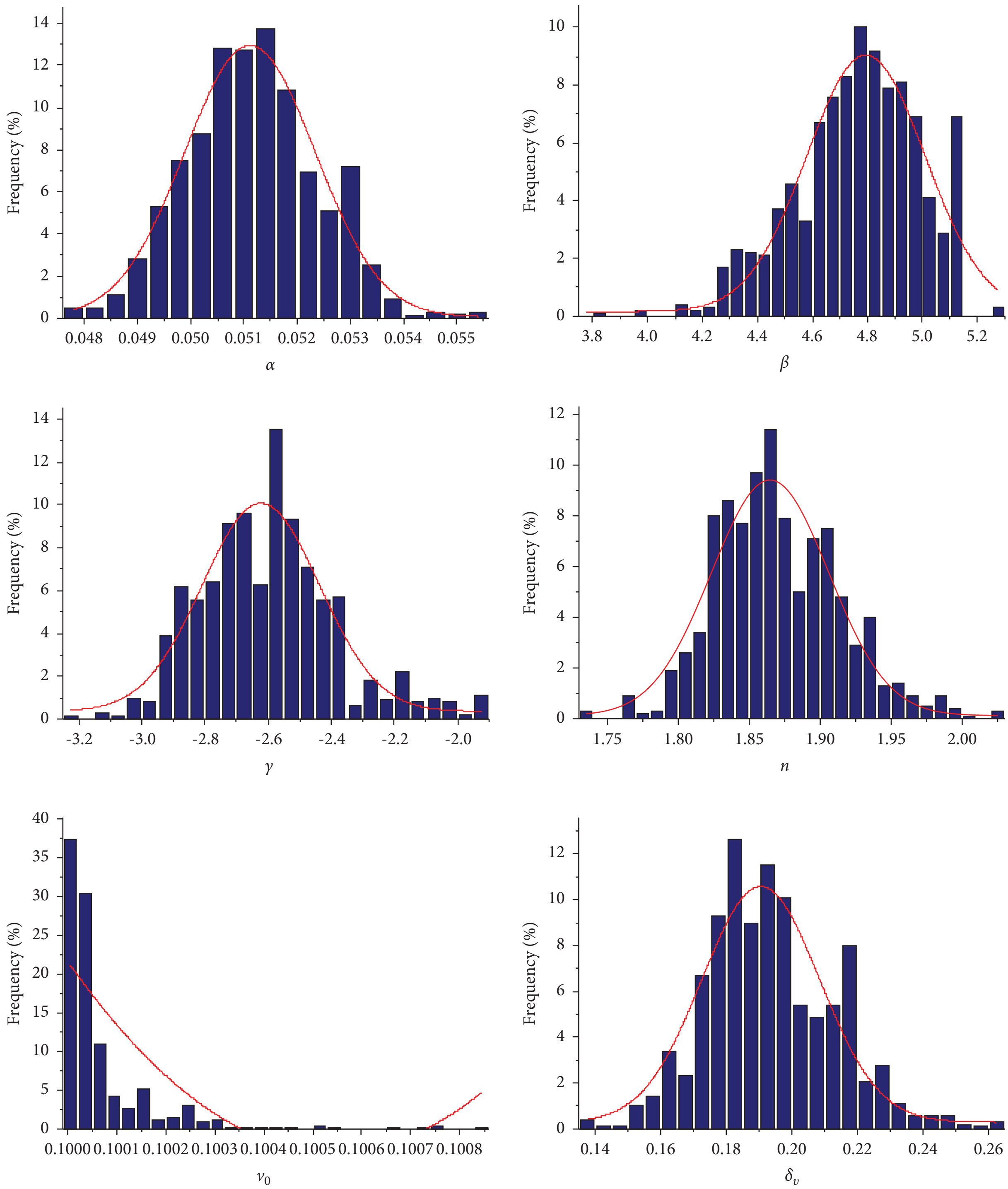

Figure 7: Continued.

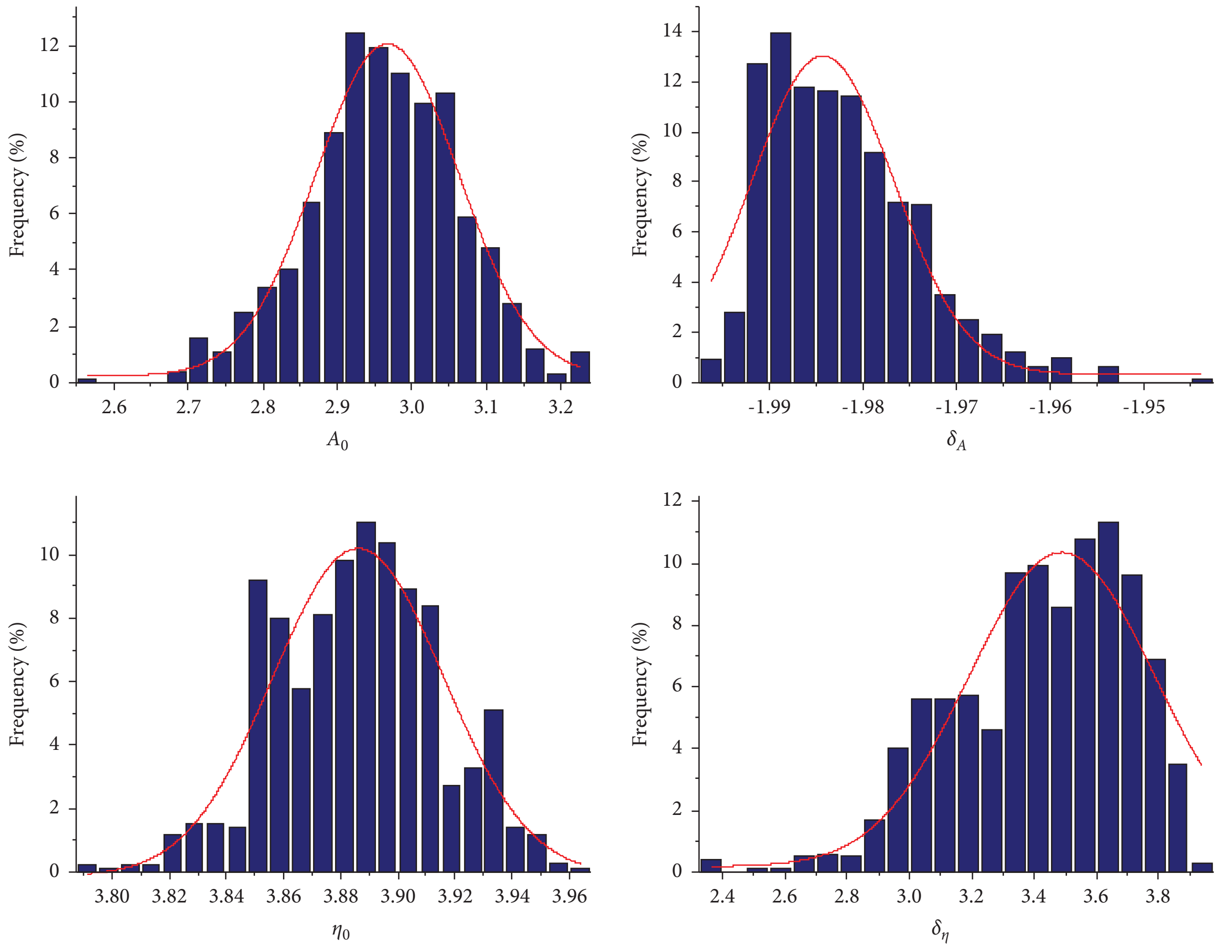

FIGURE 7: Probability distribution of each parameter.

Comparing Figures 8 and 9, it can be seen that the accuracy of the parameters taken into the model response under the sampling at a larger boundary is significantly higher than that under the sampling at a smaller boundary because of the strong correlation between the parameters [15]. Therefore, the parameter identification of the BWBN model is a global identification task, and the random sampling method may fall into a local trap. Through the iTMCMC method, adaptive selection of target distribution scale of MCMC algorithm can deal with this problem well. Using iTMCMC sampling method to estimate BWBN model parameters also has the advantage of higher efficiency. The whole calculation process is about five minutes, which is greatly improved compared with the traditional Bayesian model updating method.

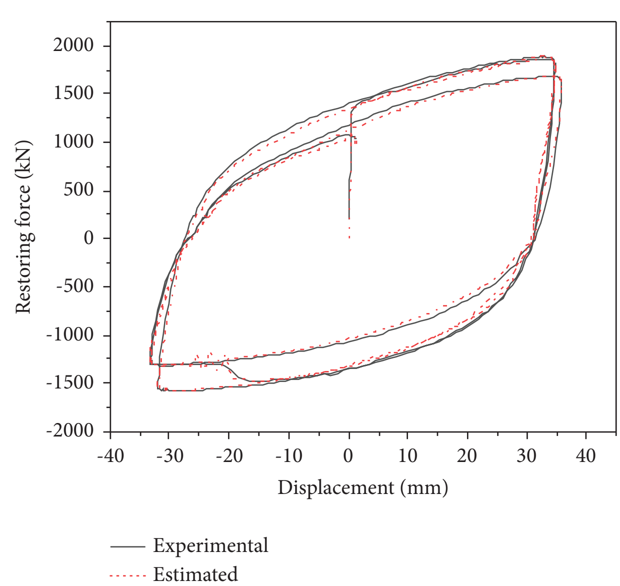

FIGURE 8: Hysteresis cycles for large range sampling parameters.

6. Example Analysis of Seismic Response

In order to carry out finite element simulation and shaking table test of earthquake simulation, a four story and four span space reinforced concrete frame model is designed in this paper. All beams and columns adopt the size

Table 2: Parameter estimation and variance.

Parameter	Estimated	Variance	Significance
α	0.051157	0.0012377	Stiffness ratio
β	4.76381	0.225278	Hysteresis area
γ	−2.59916	0.216215	Plumpness parameter
n	1.8705	0.0437203	Smoothness parameter of the model
v_0	0.100063	$9.53017e-05$	Strength degradation
δ_v	0.193383	0.0196162	Strength degradation
A_0	2.96138	0.10239	Strength and stiffness degradation
δ_A	−1.98218	0.0080262	Strength and stiffness degradation
η_0	3.88594	0.0287953	Stiffness degradation
δ_η	3.42436	0.280545	Stiffness degradation

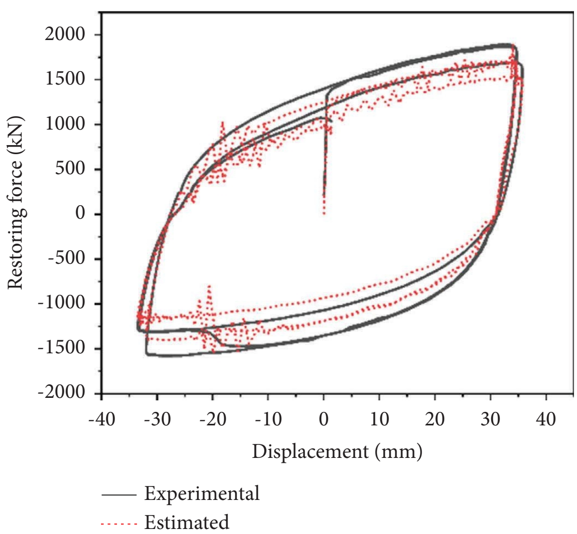

Figure 9: Hysteresis cycles for small range sampling parameters.

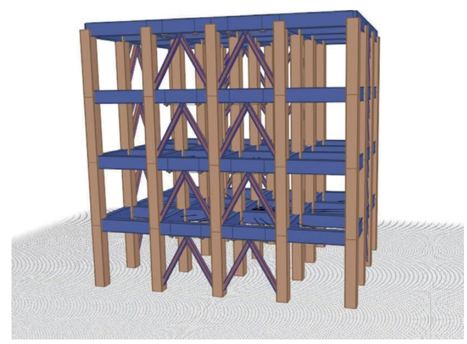

Figure 10: Model diagram.

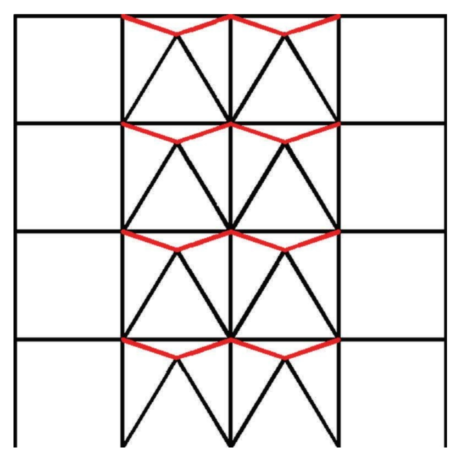

Figure 11: Model diagram.

of 18@100, Steel 02 constitutive model is selected for reinforcement, and the cross-section of the beam is 300 mm × 600 mm, the cross-section of the column is 500 mm × 500 mm, the concrete constitutive model is concrete01 constitutive model, and the restraint effect of transverse stirrup is considered for the core concrete. In order to consider the crushing phenomenon of the concrete in the protective layer, the ultimate strength of the concrete in the protective layer is taken as 30% of the peak strength of the concrete, and the ultimate strain is taken as 0.006. A uniformly distributed load of 10 kN/m is applied to each beam, and the mass of each floor is simplified to the node mass of 50 t. The BRB members are simulated by the BWBN material constitution in OpenSees, and the seismic effect is simulated by applying the inertial force on the base, and a four-story reinforced concrete frame structure is established, STKO model is shown in Figures 10 and 11.

According to the seismic influence coefficient curve of building structure, Tabas wave and El Centro wave are respectively adopted in this paper, and the peak acceleration of seismic wave is taken as 0.1 g, 0.2 g, and 0.25 g through amplitude modulation, and only the seismic wave x is input in the form of bottom inertial force. The ideal elastic-plastic model is adopted to consider the effect of rigid floor. Specific seismic waves are shown in Figures 12 and 13.

Under the action of earthquake, the BRB member makes the main structure basically in the elastic range by yielding energy dissipation, to avoid the damage to the main member. Because there are many dampers arranged in this paper, the force in the damper is small under small acceleration, and a relatively complete hysteresis loop cannot be formed. Figure 14 show the hysteresis curves of the dampers of the first to fourth layers under 0.25 g seismic wave.

It can be seen from the figure that the unloading stiffness and the initial stiffness of the damper are almost the same, which is also in line with the experimental results. At the same time, the yield layer of BRB can be obtained through analysis, and the effect of each layer of dampers under moderate earthquakes can be seen. This can effectively guide

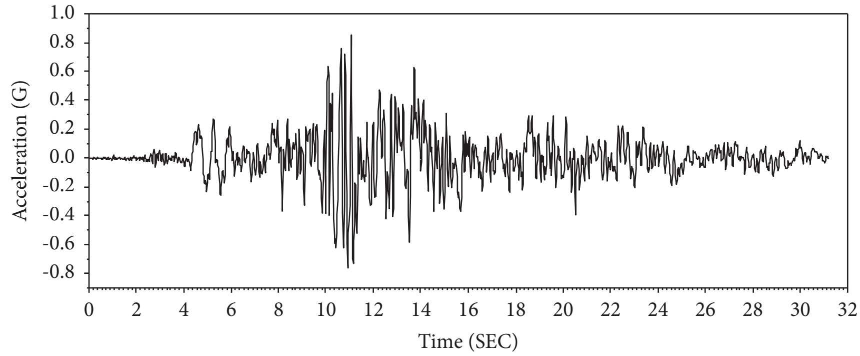

FIGURE 12: Tabas, Iran 09/16/78 seismic wave.

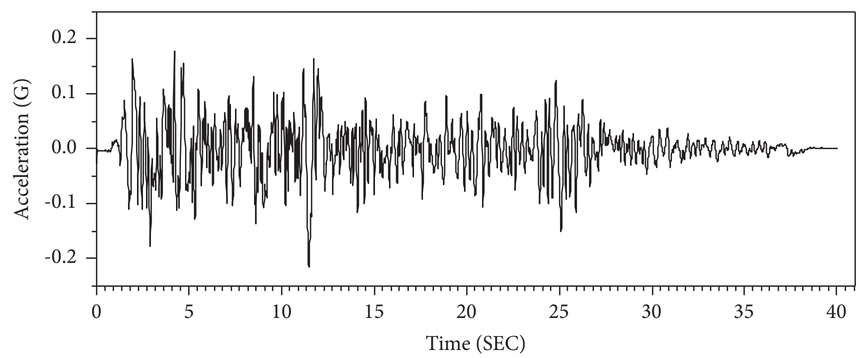

FIGURE 13: EI centro 270 seismic wave.

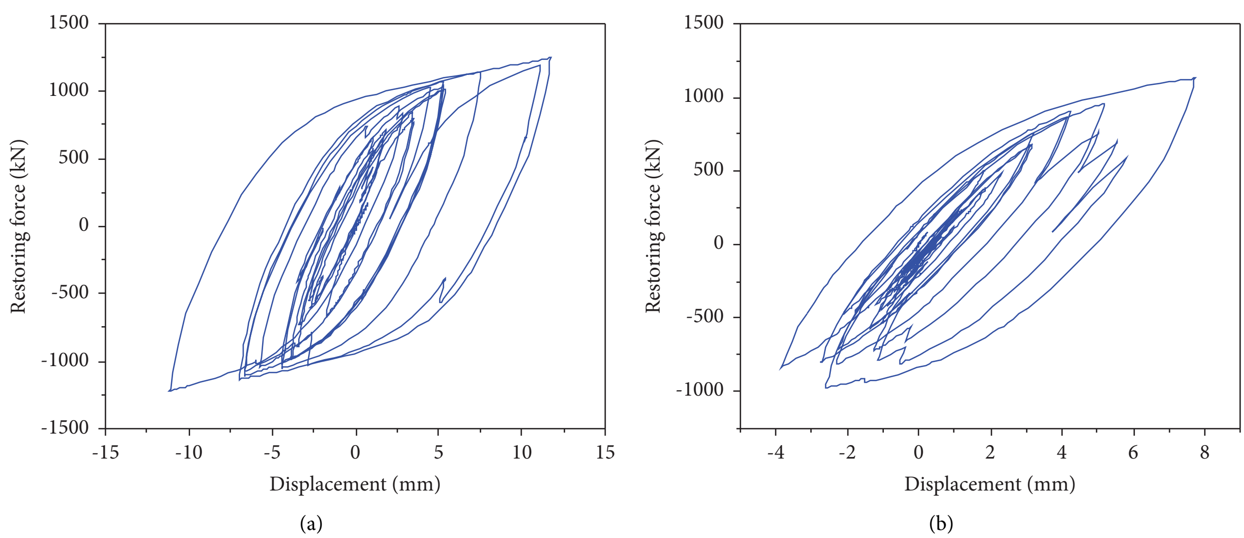

FIGURE 14: Continued.

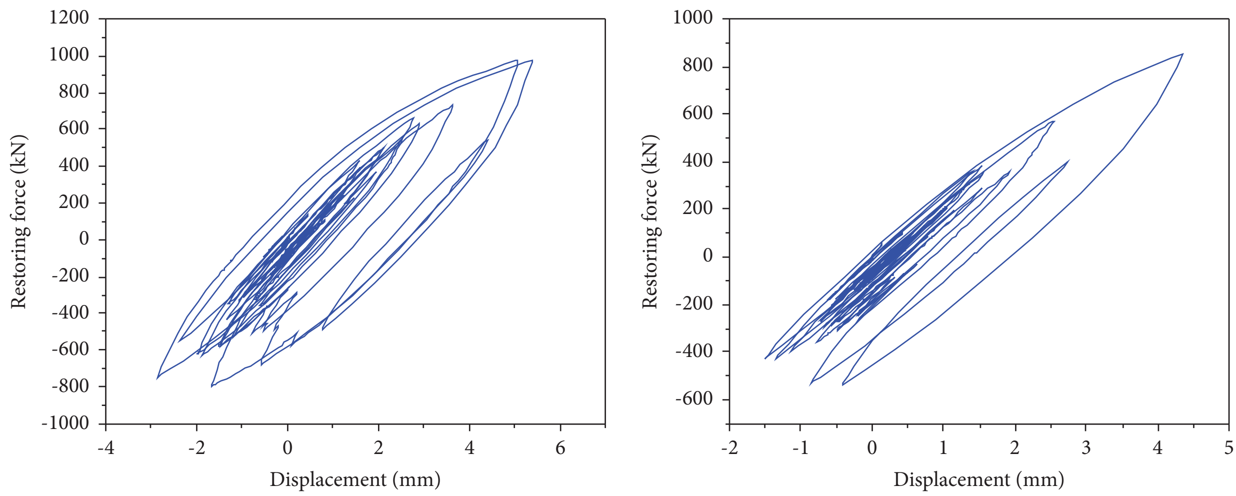

(c) (d)

Figure 14: Hysteresis cycles of dampers under TABAS seismic waves. (a) First floor. (b) Second floor. (c) Third floor. (d) Fourth floor.

the design and arrangement of dampers, and has strong engineering practical significance. The horizontal stiffness and bearing capacity of the empty frame are low, and the energy dissipation capacity is poor. However, the BRB reinforced frame has better seismic resistance. The horizontal force displacement hysteresis curve of the new double order buckling restrained brace in the structure is full and stable.

7. Conclusion

In order to determine the relationship between the force and deformation of the buckling restrained brace, a new iTMCMC method is adopted to identify the parameters of the improved BW model, and then the parameters are brought into the BW material constitutive model of OpenSees to obtain the response of the new double-order buckling restrained brace under the actual earthquake, to realize the simulation of the application of new materials in the structure. This paper mainly obtains the following conclusions:

(i) The iTMCMC method is successfully applied to the parameter identification of the improved BW model lag model. The identification method has shown its ability to find a parameter set that can accurately reproduce the system response.

(ii) In the analysis model of BRB reinforced concrete frame, the improved BW model constitutive element is adopted for the BRB frame, and the inertial force at the bottom is considered for the seismic action of the structure. The numerical analysis results of reinforced concrete frame show that the simulation results are in good agreement with the test results. The reinforced concrete frame analysis model can accurately predict the seismic performance of empty frame and BRB reinforced frame.

(iii) The improved BW model can better simulate the hysteresis characteristics of BRB. Compared with the classical BW model, it can better reflect the characteristics of plastic hardening of materials and asymmetry of mechanical parameters, to guide the design and engineering arrangement of dampers.

(iv) In view of the results of numerical experiments, the proposed iTMCMC method should be applied to other hysteresis models, such as biaxial models or asymmetric hysteresis models, to evaluate the efficiency of the algorithm in dealing with other nonlinear hysteresis models.

Data Availability

The data used to support the findings of this study have been deposited in the repository ((ZHAO, Lu (2022): data in paper. figshare. Journal contribution. https://doi.org/10.6084/m9.figshare.21086056.v1)).

Conflicts of Interest

The authors declare that they have no conflicts of interest.

Acknowledgments

Shanghai Municipal Fund Project for Central Guiding Local Science and Technology Development (YDZX20223100003003).

References

[1] Y.-F. Jin, Z.-Y. Yin, Z.-X. Wu, and A. Daouadji, "Numerical modeling of pile penetration in silica sands considering the effect of grain breakage," *Finite Elements in Analysis and Design*, vol. 144, pp. 15–29, 2018.

[2] Y.-F. Jin, Z.-Y. Yin, Z.-X. Wu, and W. H. Zhou, "Identifying parameters of easily crushable sand and application to off-shore pile driving," *Ocean Engineering*, vol. 154, pp. 416–429, 2018.

[3] C.-H. Loh, C.-H. Mao, J.-R. Huang, and T. C. Pan, "System identification and damage evaluation of degrading hysteresis of reinforced concrete frames," *Earthquake Engineering & Structural Dynamics*, vol. 40, no. 6, pp. 623–640, 2011.

[4] K. Goda, H. P. Hong, and C. S. Lee, "Probabilistic characteristics of seismic ductility demand of SDOF systems with b-wen hysteretic behavior," *Journal of Earthquake Engineering*, vol. 13, no. 5, pp. 600–622, 2009.

[5] C. L. Ning, Y. Cheng, and X. H. Yu, "A simplified approach to investigate the seismic ductility demand of shear-critical reinforced concrete columns based on experimental calibration," *Journal of Earthquake Engineering*, vol. 25, no. 10, pp. 1958–1980, 2021.

[6] Z. Li, M. Noori, Y. Zhao, C. Wan, D. Feng, and W. A. Altabey, "A multi-objective optimization algorithm for Bouc–Wen–Baber–Noori model to identify reinforced concrete columns failing in different modes," *Proceedings of the Institution of Mechanical Engineers - Part L: Journal of Materials: Design and Applications*, vol. 235, no. 9, pp. 2165–2182, 2021.

[7] A. Silik, M. Noori, W. A. Altabey, and R. Ghiasi, "Selecting optimum levels of wavelet multi-resolution analysis for time-varying signals in structural health monitoring," *Structural Control and Health Monitoring*, vol. 28, no. 8, 2021.

[8] Z. Y. Li, F. Albermani, R. W. K. Chan, and S. Kitipornchai, "Pinching hysteretic response of yielding shear panel device," *Engineering Structures*, vol. 33, no. 3, pp. 993–1000, 2011.

[9] A. Bahar, F. Pozo, L. Acho, J. Rodellar, and A. Barbat, "Hierarchical semi-active control of base-isolated structures using a new inverse model of magnetorheological dampers," *Computers & Structures*, vol. 88, no. 7-8, pp. 483–496, 2010.

[10] P. Sengupta and B. Li, "Modified Bouc–Wen model for hysteresis behavior of RC beam–column joints with limited transverse reinforcement," *Engineering Structures*, vol. 46, pp. 392–406, 2013.

[11] P. Sengupta and B. Li, "Hysteresis behavior of reinforced concrete walls," *Journal of Structural Engineering*, vol. 140, no. 7, 2014.

[12] R. Rosli, M. Z. Mohamed, G. Priyandoko, and M. F. F. A. Rashid, "Bouc-wen hysteresis parameter optimization for magnetorheological damper using Cuckoo Search algorithm," in *Proceedings of the 2019 4th International Conference on the Science and Engineering of Materials (ICoSEM)*, Kyoto, Japan, October 2020.

[13] S. L. Xie, Y. H. Zhang, C. H. Chen, and X. Zhang, "Identification of nonlinear hysteretic systems by artificial neural network," *Mechanical Systems and Signal Processing*, vol. 34, no. 1-2, pp. 76–87, 2013.

[14] G. A. Ortiz, D. A. Alvarez, and D. Bedoya-Ruíz, "Identification of Bouc-Wen type models using the Transitional Markov chain Monte Carlo method," *Computers & Structures*, vol. 146, pp. 252–269, 2015.

[15] G. A. Ortiz, D. A. Alvarez, and D. Bedoya-Ruiz, "Identification of Bouc–Wen type models using multi-objective optimization algorithms," *Computers & Structures*, vol. 115, pp. 121–132, 2013.

[16] D. De Domenico, G. Ricciardi, and I. Takewaki, "Design strategies of viscous dampers for seismic protection of building structures: a review," *Soil Dynamics and Earthquake Engineering*, vol. 118, pp. 144–165, 2019.

[17] I. Takewaki and H. Akehashi, "Comprehensive review of optimal and smart design of nonlinear building structures with and without passive dampers subjected to earthquake loading," *Frontiers in Built Environment*, vol. 7, 2021.

[18] H. Akehashi and I. Takewaki, "Bounding of earthquake response via critical double impulse for efficient optimal design of viscous dampers for elastic-plastic moment frames," *Japan Architectural Review*, vol. 5, no. 2, pp. 131–149, 2022.

[19] J. W. Hu, M. H. Noh, and J. H. Ahn, "Experimental investigation on the behavior of bracing damper systems by utilizing metallic yielding and r material devices," *Advances in Materials Science and Engineering*, vol. 2018, Article ID 2813058, 15 pages, 2018.

[20] M. Mohammadi, M. A. Kafi, A. Kheyroddin, and H. R. Ronagh, "Experimental and numerical investigation of an innovative buckling-restrained fuse under cyclic loading," *Structures*, vol. 22, pp. 186–199, 2019.

[21] F. Rezazadeh and S. Talatahari, "Seismic energy-based design of BRB frames using multi-objective vibrating particles system optimization," *Structures*, vol. 24, pp. 227–239, 2020.

[22] J. Zhao, X. Sun, and L. Huo, "Seismic performance of concrete frame structures with buckling-restrained brace," *China Earthquake Engineering Journal*, vol. 37, no. 1, pp. 100–105, 2015.

[23] R. Tremblay, P. Bolduc, R. Neville, and R. DeVall, "Seismic testing and performance of buckling-restrained bracing systems," *Canadian Journal of Civil Engineering*, vol. 33, no. 2, pp. 183–198, 2006.

[24] C. L. Wang, T. Usami, J. Funayama, and F. Imase, "Low-cycle fatigue testing of extruded aluminium alloy buckling-restrained braces," *Engineering Structures*, vol. 46, pp. 294–301, 2013.

[25] H. Akehashi and I. Takewaki, "Resilience evaluation of elastic-plastic high-rise buildings under resonant long-duration ground motion," *Japan Architectural Review*, vol. 5, no. 4, pp. 373–385, 2022.

[26] T. T. Baber and Y. K. Wen, "Random vibration of hysteretic, degrading systems," *Journal of the Engineering Mechanics Division*, vol. 107, no. 6, pp. 1069–1087, 1981.

[27] T. T. Baber and M. N. Noori, "Random vibration of degrading, pinching systems," *Journal of Engineering Mechanics*, vol. 111, no. 8, pp. 1010–1026, 1985.

[28] K. Worden and J. J. Hensman, "Parameter estimation and model selection for a class of hysteretic systems using Bayesian inference," *Mechanical Systems and Signal Processing*, vol. 32, pp. 153–169, 2012.

[29] M. Cheng, Y. Jin, Z. Yin, and S. Horpibulsuk, "Enhanced DE-TMCMC and its application in identifying parameters of advanced soil model," *Chinese Journal of Geotechnical Engineering*, vol. 41, no. 12, pp. 2281–2289, 2019.

[30] W. Betz, I. Papaioannou, and D. Straub, "Transitional Markov chain Monte Carlo: observations and improvements," *Journal of Engineering Mechanics*, vol. 142, no. 5, 2016.

[31] E. Afsar Dizaj, N. Fanaie, and A. Zarifpour, "Probabilistic seismic demand assessment of steel frames braced with reduced yielding segment buckling restrained braces," *Advances in Structural Engineering*, vol. 21, no. 7, pp. 1002–1020, 2018.

[32] M. Iwata, M. Midorikawa, and K. Koyano, “Buckling-restrained brace with high structural performance,” *Steel Construction*, vol. 11, no. 1, pp. 3–10, 2018.
[33] Q. Yang, Q. Sun, W. Yang, Q. Hao, X. Wang, and B. Zhang, “Correlation between microstructure evolution and mechanical response in a moderately low stacking-fault-energy austenitic Fe–Mn–Si–Al alloy during low-cycle fatigue deformation,” *Materials Science and Engineering A*, vol. 824, Article ID 141766, 2021.
[34] W. H. Robinson and A. G. Tucker, “Test -results for lead-rubber bearings for -Wm. Clayton Building, Toe Toe Bridge and Waiotukupuna Bridge,” *Bulletin of the New Zealand Society for Earthquake Engineering*, vol. 14, no. 1, pp. 21–33, 1981.
[35] P. S. Patwardhan, R. A. Nalavde, and D. Kujawski, “An estimation of ramberg-osgood constants for materials with and without luder’s strain using yield and ultimate strengths,” in *Proceedings of the 3rd International Conference on Structural Integrity (ICSI)*, pp. 750–757, Funchal, Portugal, September 2019.
[36] Y. K. Wen, “Method for random vibration of hysteretic systems,” *Journal of the Engineering Mechanics Division*, vol. 102, no. 2, pp. 249–263, 1976.
[37] P. Angelikopoulos, C. Papadimitriou, and P. Koumoutsakos, “X-TMCMC: adaptive kriging for Bayesian inverse modeling,” *Computer Methods in Applied Mechanics and Engineering*, vol. 289, pp. 409–428, 2015.
[38] G. C. Foliente, “Hysteresis modeling of wood joints and structural systems,” *Journal of Structural Engineering*, vol. 121, no. 6, pp. 1013–1022, 1995.
[39] N. Chao-Lie, Y. Cheng, and X. Yu, “A simplified approach to investigate the seismic ductility demand of shear-critical reinforced concrete columns based on experimental calibration,” *Journal of Earthquake Engineering*, vol. 25, 2019.